

# Polarized infrared spectroscopic study on the orientation of the molecules in the smectic- $C^*$ phase of a ferroelectric liquid crystal with a naphthalene ring: Alternative theory for the analysis of polarization-angle-dependent intensity changes

J. G. Zhao,<sup>1</sup> T. Yoshihara,<sup>2</sup> H. W. Siesler,<sup>3</sup> and Y. Ozaki<sup>1,\*</sup>

<sup>1</sup>*Department of Chemistry, School of Science, Kwansei-Gakuin University, Uegahara, Nishinomiya 662-8501, Japan*

<sup>2</sup>*Display Laboratories, Fujitsu Laboratories Limited, Ohkubo, Akashi 674-0054, Japan*

<sup>3</sup>*Department of Physical Chemistry, University of Essen, D-45117 Essen, Germany*

(Received 7 February 2001; published 21 August 2001)

A theory to explain the polarization-angle dependence of polarized infrared spectra of a ferroelectric liquid crystal in the surface-stabilized ferroelectric liquid crystal state is proposed. It describes the relationship between the intensity of the absorption bands and the polarization angle of the infrared radiation. Using this theory the polarization-angle dependence of the infrared band intensities was analyzed for a ferroelectric liquid crystal with a naphthalene ring and two phenyl rings with a stacked layer structure in the smectic- $C^*$  phase. The polarization-angle-dependent spectra were measured at 137 °C under external dc electric fields of +40 and -40 V to investigate the orientation of the molecules. Plots of the infrared absorbance versus polarization angle for representative bands were subjected to a curve fitting procedure by a least squares method. From the curves obtained the orientation of the transition dipole moments with respect to the molecular long axis and the orientation of the molecular long axis with respect to the rubbing direction of the cell were estimated based upon the suggested theory. The polarization-angle-dependent infrared spectra obtained were also analyzed by two-dimensional (2D) correlation spectroscopy. The 2D correlation analysis clearly detects a slight phase difference in the polarization-angle dependence which is hardly recognized in ordinary plots of the intensity changes in the infrared bands. The 2D correlation analysis allows us to separate asymmetric and symmetric stretching bands due to the chiral methyl group from those arising from other methyl groups in the alkyl chains.

DOI: 10.1103/PhysRevE.64.031704

PACS number(s): 61.30.Eb

## I. INTRODUCTION

The ferroelectric smectic- $C^*$  (Sm- $C^*$ ) phase was discovered in 1975 and proved to have a unique form of ferroelectricity [1,2]. Five years passed before a technical application of this effect was first suggested. Clark and Lagerwall [3] proposed the use of a very thin cell to make the boundary conditions imposed by the orientation layers strong enough to suppress the helix; this is called the surface-stabilized ferroelectric liquid crystal (SSFLC) effect. Ferroelectric liquid crystal molecules have a permanent electric dipole perpendicular to their molecular long axis. By changing the polarity of the external applied electric field, the permanent electric dipole will rotate by 180° to point in the opposite direction; the molecular long axis can switch between the two SSFLC states. As the macroscopic geometry of the SSFLC effect has been clarified [4–6], investigations of the microscopic mechanism of the electric-field-induced reorientation of the alkyl chain, the mesogen, and other segments of the ferroelectric liquid crystals have become more and more frequent [7].

During the past decade polarization infrared spectroscopy and time-resolved infrared spectroscopy have been applied as powerful tools for investigating the static orientation and dynamic behavior of liquid crystalline molecules [8–31]. Po-

larization infrared spectroscopy can be used to provide information about the direction of transition dipole moments of the normal modes of vibrations. Measurement of the polarization-angle dependence of infrared bands of a ferroelectric liquid crystal in the Sm- $C^*$  phase is very useful in exploring its molecular structure and alignment. However, the analysis of the polarization-angle dependence of infrared band intensity is not always straightforward, partly because some of the bands may overlap each other and partly because some may show very similar polarization-angle dependence. Thus it is of importance to establish the theoretical relationship between the infrared absorbance and the polarization angle for studies of the orientation of liquid crystal molecules. With this relationship, one can not only analyze precisely the dependence of the absorbance upon the polarization angle, but also gain information concerning the angle between the transition moment and the molecular long axis. Two models [32] have been developed for this theoretical relationship. One is based on the statistical average of the absorption of individual dipolar moments with an orientation distribution described by a series of spherical harmonics. Because this model is established only for individual dipolar moments, it cannot offer information about the angle between the transition moment and the molecular long axis. The other model is built on the basis of classic polarization theory. However, this model does not take into account the contribution from nonpolarization components to the IR absorbance, and it also cannot offer information concerning the angle between the transition moment and the molecular long axis.

\*Author to whom correspondence should be addressed. Present address: School of Science, Kwansei Gakuin University, Nishinomiya 662-8501, Japan. Email address: ozaki@kwansei.ac.jp

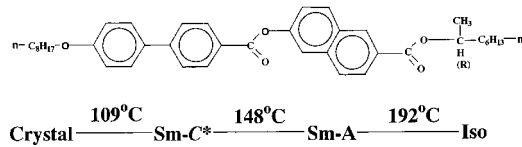


FIG. 1. Structure of FLC-3 and the phase transition temperature.

In the present study, we propose an alternative theory for analyzing the polarization-angle dependences in more detail. This theory describes the relationship between the band intensities and the polarization angle of the infrared radiation. The theory also allows us to investigate quantitatively the orientation angle of the molecular long axis with respect to the polarization direction at  $0^\circ$  and with respect to the rubbing direction, and the mean orientation angle of a transition dipole moment with respect to the direction of the molecular long axis. This information about the angles is particularly useful for studying the relationship between the molecular structure and the alignment of a ferroelectric liquid crystal. The theory also shows that the polarization-angle-dependent features of bands with an orientation angle less than the magic angle ( $54.7^\circ$ ) will be diametrically opposed to those with an orientation angle larger than the magic angle. Furthermore, on the basis of the theory the average direction of the molecular long axis can be determined with improved accuracy from the absorbance at varying polarization angles.

In the present study we also use generalized two-dimensional (2D) correlation spectroscopy [33] to analyze the polarization-angle dependence of infrared band intensities. In a typical 2D correlation analysis, a series of perturbation-induced dynamic spectra are collected as a function of the quantitative measure of the imposed physical effect itself [34–36]. In our previous paper [30], we demonstrated the potential of 2D correlation spectroscopy for analysis of the polarization-angle dependence of infrared band intensity. In 2D correlation infrared spectroscopy of polarization-angle-dependent spectral changes [30], no perturbation is imposed upon the sample itself; the polarization angle is used as the perturbation. The 2D correlation analysis allows one to detect slight differences in the polarization-angle dependence. Moreover, it enhances the spectral resolution, deconvoluting overlapped bands.

The purpose of the present study is to provide deeper insight into the structure and alignment of molecular segments in a ferroelectric liquid crystal with a naphthalene ring and two phenyl rings (FLC-3; Fig. 1) using both the theory presented here and 2D correlation analysis.

## II. THEORY

In previous studies on ferroelectric liquid crystals the relative orientation of an alkyl chain, a mesogen, and a chiral segment were investigated by IR polarization spectroscopy. In the present study a quantitative analysis of the polarization-angle dependence of the infrared band intensities of FLC-3 is performed. We have attempted to derive a model for the relationship between the absorbance of the IR

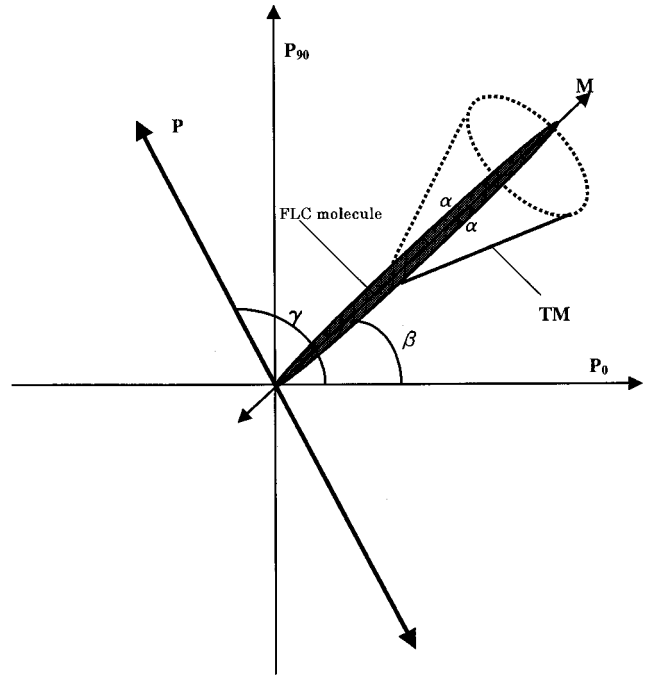


FIG. 2. Schematic model of the relative positions of the polarization directions ( $P_0$ ,  $P_{90}$ , and  $P$ ), the transition moment (TM), and the molecular long axis ( $M$ ).  $P_0$  is the polarization direction of the incoming beam at  $0^\circ$  polarizer setting.  $P_{90}$  is the polarization direction of the incoming beam at  $90^\circ$  polarizer setting.  $P$  is the polarization direction of an arbitrary polarizer setting making an angle  $\gamma$  with  $P_0$ .  $M$  is the molecular long axis of the investigated FLC in the plane ( $P_0, P_{90}$ ) and makes an angle  $\beta$  with  $P_0$ . TM lies at the intersection of the plane ( $P_0, P_{90}$ ) with the cone made by the transition moment around  $M$  (opening angle  $\alpha$ ).

bands and the polarization angle of the IR radiation. In this model the transition dipole moment of the absorption band investigated lies on a cone with semiangle  $\alpha$  around the molecular long axis of the ferroelectric liquid crystal. Figure 2 shows a model of the relative positions of the molecular long axis, the transition dipole moment, and the polarization directions. For perfect uniaxial orientation  $\alpha$  is related to the polarization intensities of the investigated absorption band by [37,38]

$$\frac{A_{\text{par}}}{A_{\text{per}}} = 2 \cot^2 \alpha, \quad (1)$$

where  $A_{\text{par}}$  and  $A_{\text{per}}$  are the absorbances measured with polarized radiation parallel and perpendicular to the direction of the molecular long axis, respectively. The ferroelectric liquid crystal is arranged with its layer structure in a stacked geometry, which is assumed to be optically uniaxial, although the Sm-C\* phase is known to be weakly biaxially oriented [39]. When a voltage is applied, the molecular long axis of the ferroelectric liquid crystal orients approximately parallel to the surface of the cell windows. Thus, if the polarization direction of the incident radiation is parallel and

perpendicular to the molecular long axis, the corresponding transmittances of an absorption band  $T_{\text{par}}$  and  $T_{\text{per}}$  are given by

$$T_{\text{par}} = e^{-2A_{\text{per}} \cot^2 \alpha} \quad (2)$$

and

$$T_{\text{per}} = e^{-A_{\text{per}}}. \quad (3)$$

It should be noted that the intensity  $I_0$  of an incident polarized IR beam equals the sum of the intensities  $I_{\text{par}}$  and  $I_{\text{per}}$  of the two beams linearly polarized parallel and perpendicular to the molecular long axis direction, respectively. Thus,  $I_0$ ,  $I_{\text{par}}$ , and  $I_{\text{per}}$  are related by the equations

$$I_0 = I_{\text{par}} + I_{\text{per}}, \quad (4)$$

$$I_{\text{par}} = I_0 \cos^2(\gamma - \beta), \quad (5)$$

$$I_{\text{per}} = I_0 \sin^2(\gamma - \beta), \quad (6)$$

where  $\gamma$  and  $\beta$  are the angles of  $P_0$  with the polarization direction  $P$  of the incident radiation and the molecular long axis direction, respectively (Fig. 2). The angle  $\beta$  is called the orientation angle of the molecular long axis. The angle  $\gamma$  is the polarization direction angle of the incident radiation and varies from  $0^\circ$  to  $180^\circ$ . The intensity  $I$  of the polarized IR radiation transmitted by the ferroelectric liquid crystal equals the sum of the transmitted intensities  $I_{\text{tpar}}$  and  $I_{\text{tper}}$  of the two beams polarized parallel and perpendicular to the molecular long axis, respectively. Considering a ferroelectric liquid crystal material with a layer structure arranged in a stacked geometry, which is assumed to be optically uniaxial,  $I$ ,  $I_{\text{tpar}}$ , and  $I_{\text{tper}}$  are given by the equations

$$I = I_{\text{tpar}} + I_{\text{tper}}, \quad (7)$$

$$I_{\text{tpar}} = I_0 e^{-2A_{\text{per}} \cot^2 \alpha} \cos^2(\gamma - \beta), \quad (8)$$

$$I_{\text{tper}} = I_0 e^{-A_{\text{per}}} \sin^2(\gamma - \beta). \quad (9)$$

The transmittance  $T$  can thus be expressed as a function of the polarization angle  $\gamma$  of the incoming radiation and the orientation angle of the molecular long axis  $\beta$  by

$$T = e^{-2A_{\text{per}} \cot^2 \alpha} \cos^2(\gamma - \beta) + e^{-A_{\text{per}}} \sin^2(\gamma - \beta), \quad (10)$$

If we consider that the ferroelectric liquid crystalline system under consideration has a two-phase structure composed of a perfectly uniaxial phase and an isotropic phase, the absorbance  $A_p$  of the ferroelectric liquid crystalline system is expressed by

$$A_p = -S \ln[e^{-2A_{\text{per}} \cot^2 \alpha} \cos^2(\gamma - \beta) + e^{-A_{\text{per}}} \sin^2(\gamma - \beta)] + B, \quad (11)$$

where  $S \geq 0$  is a constant that represents the contribution of a perfectly uniaxial phase to  $A_p$ .  $B$  is dependent on the contribution of the isotropic phase. When  $\cot^2 \alpha = 0.5$  ( $\alpha$

$= 54.7^\circ$ ), the ferroelectric liquid crystalline system is a perfectly isotropic phase because according to Eq. (1)  $A_{\text{per}} = A_{\text{par}}$  and  $A_p$  becomes  $A_{\text{iso}}$ . Therefore,  $B$  can be expressed as

$$B = (1 - S)A_{\text{iso}}. \quad (12)$$

Consequently, Eq. (11) can be replaced by the equations

$$A_p = -S \ln[e^{-2A_{\text{per}} \cot^2 \alpha} \cos^2(\gamma - \beta) + e^{-A_{\text{per}}} \sin^2(\gamma - \beta)] + (1 - S)A_{\text{iso}}, \quad (13)$$

where  $A_{\text{iso}}$  is the absorbance of an absorption band for a perfectly isotropic phase. The physical meaning of  $S$  and  $1 - S$  is the proportion of molecules in the perfectly uniaxial phase and in the isotropic phase of the ferroelectric liquid crystalline system, respectively.

To obtain a relationship between each polarization direction angle  $\gamma$  of the incoming beam and the orientation angle of the molecular long axis,  $\beta$ , the first and second derivatives of  $A_p$  with respect to  $\gamma$  have been calculated for Eq. (13):

$$\frac{\partial A_p}{\partial \gamma} = C \sin[2(\gamma - \beta)](e^{-A_{\text{per}}} - e^{-2A_{\text{per}} \cot^2 \alpha}), \quad (14)$$

$$\begin{aligned} \frac{\partial^2 A_p}{\partial \gamma^2} &= 2C \cos[2(\gamma - \beta)](e^{-A_{\text{per}}} - e^{-2A_{\text{per}} \cot^2 \alpha}) \\ &+ \frac{C^2}{S} \sin^2[2(\gamma - \beta)](e^{-A_{\text{per}}} - e^{-2A_{\text{per}} \cot^2 \alpha})^2, \end{aligned}$$

$$C = -\frac{S}{e^{-2A_{\text{per}} \cot^2 \alpha} \cos^2(\gamma - \beta) + e^{-A_{\text{per}}} \sin^2(\gamma - \beta)}, \quad (15)$$

where  $C \leq 0$ . When  $\gamma = \beta$  and  $\alpha < 54.7^\circ$ , the absorbance will be a maximum in the polarization direction parallel to the direction of the molecular long axis, and we can obtain the value of the orientation angle of the molecular long axis,  $\beta$ . When  $\gamma = \beta \pm \pi/2$  and  $\alpha > 54.7^\circ$ , the absorbance will be a maximum in the polarization direction perpendicular to the direction of the molecular long axis, and we can also obtain the value of the orientation angle of the molecular long axis,  $\beta$ .  $A_p$  and  $A_{\text{iso}}$  were usually transformed to a logarithm with base 10 by dividing both sides of Eq. (13) by  $\ln 10$ . Then we applied a curve fitting procedure by a least squares method for the typical bands and thereby obtained the  $\beta$ ,  $\alpha$ , and  $S$  values for the system under investigation.

Now we define a normalized absorbance as follows:

$$A_{n-p} = \frac{A_p - A_{\text{min}}}{A_{\text{max}} - A_{\text{min}}}, \quad (16)$$

where  $A_{\text{max}}$  and  $A_{\text{min}}$  are the maximum and the minimum, respectively, of  $A_p$ . According to Eq. (13) we obtain a normalized absorbance for  $\alpha < 54.7^\circ$ :

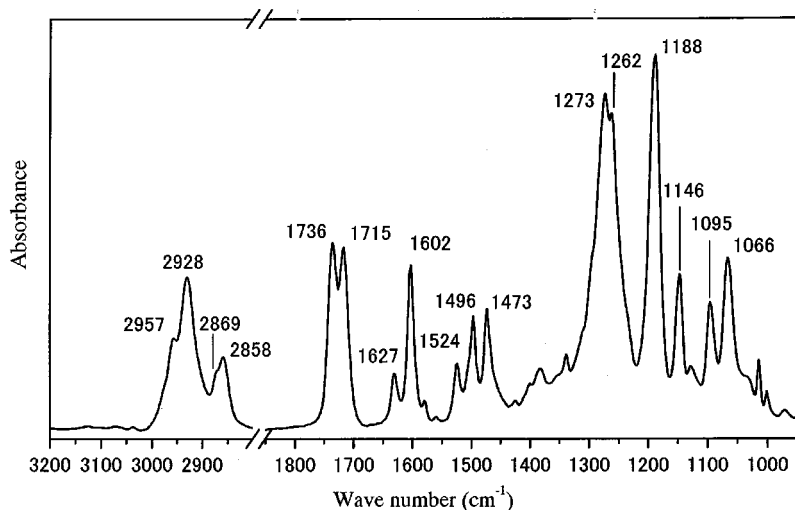


FIG. 3. Infrared spectrum of FLC-3 in the Sm-C\* phase at 137 °C.

$$A_{n-p} = \frac{1 + (1/A_{per}) \ln[e^{-2A_{per} \cot^2 \alpha} \cos^2(\gamma - \beta) + e^{-A_{per} \sin^2(\gamma - \beta)}]}{1 - 2 \cot^2 \alpha} \quad (17)$$

and for  $\alpha > 54.7^\circ$

$$A_{n-p} = \frac{2 \cot^2 \alpha + (1/A_{per}) \ln[e^{-2A_{per} \cot^2 \alpha} \cos^2(\gamma - \beta) + e^{-A_{per} \sin^2(\gamma - \beta)}]}{2 \cot^2 \alpha - 1} \quad (18)$$

In the case of a normalized absorbance with  $1 \geq A_{n-p} \geq 0$ ,  $A_{n-p}$  is independent of  $S$  and  $A_{iso}$ .

### III. EXPERIMENT

The chemical structure along with the phase transition temperatures of the investigated ferroelectric liquid crystal

TABLE I. Dichroic ratio ( $D$ ) and band assignments for the relevant peaks in the infrared spectra of FLO-3 in the Sm-C\* phase.

Wave number (cm <sup>-1</sup> )	Assignment <sup>a</sup>	Dichroic ratio $D$
2957	CH <sub>3</sub> asym. st.	0.85
2928	CH <sub>2</sub> antisym. st.	0.82
2869	CH <sub>3</sub> sym. st.	0.95
2858	CH <sub>2</sub> sym. st.	0.81
1736	C=O st. (core)	0.66
1715	C=O st. (chiral)	0.80
1627	ring C=C st.	1.94
1602	ring C=C st.	9.94
1524	ring C=C st.	6.19
1496	ring C=C st.	5.92
1473	CH <sub>2</sub> scissoring	3.77
1273		6.78
1262	C—O—C antisym. st.	8.00
1188	C—O—C antisym. st.	9.53
1146	C—O—C sym. st.	6.84
1095	C—O—C sym. st. (chiral)	4.84
1066	C—O—C sym. st.	3.31

<sup>a</sup>Sym. indicates symmetric, asym. asymmetric, antisym. antisymmetric, and st. stretching.

FLC-3 are shown in Fig. 1. The synthesis of this liquid crystal was reported in Ref. [40]. The sample cell consisted of two BaF<sub>2</sub> plates coated with conducting layers of indium tin oxide and polyamide rubbed in one direction. The thickness between the two plates, as determined from the interference fringe pattern, was adjusted to 1.7 μm with a silicone spacer. The cell was filled with molten sample by capillary action, heated to the isotropic phase, and then slowly cooled down to a temperature in the Sm-C\* phase. Temperature was controlled to an accuracy of ±0.05 °C with the aid of a Mettler

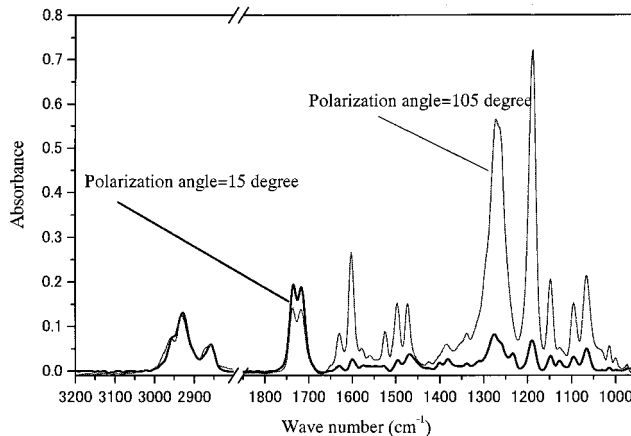


FIG. 4. Polarization infrared spectra of FLC-3 in the parallel (105°) and perpendicular (15°) polarization geometries.



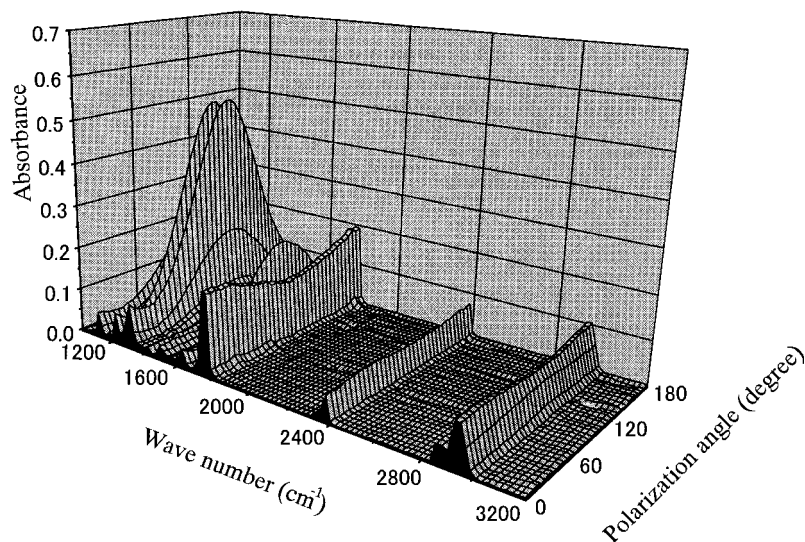


FIG. 5. Polarization-angle dependence of polarized infrared spectra of FLC-3 in the Sm-C\* phase at 137 °C under an external dc electric field of -40 V.

FP80HT thermocontroller. The approximate size of the domain was in the several hundred micrometer range.

IR polarization spectra were measured on a well aligned domain of the sample with a Jeol Model JIR-6500 FTIR spectrometer equipped with a Jeol Model IR-MAU 100 microattachment and a mercury-cadmium-tellurium detector. A wire grid polarizer was rotated about the axis parallel to the propagation direction of the incident IR radiation.

IR polarization spectra were measured under dc applied voltages of 40 V of both polarities at 137 °C. The polarization angles were read directly from the dial of the polarizer. The spectra obtained were corrected for baseline using a nonlinear spline function, and bands arising from the water vapor in the spectrometer were subtracted. In order to separate the overlapping bands, the IR spectra were curve fitted using the GRAMS program, and the areas and heights of the separated bands were used for further processing of the data.

The synchronous and asynchronous spectra were calculated based upon an algorithm recently developed by Noda *et al.* [41] and used in a software program named 2D POCHA [42].

#### IV. RESULTS AND DISCUSSION

##### A. Band assignments and measurements of dichroic ratio

Figure 3 shows an infrared spectrum of FLC-3 in the Sm-C\* phase at 137 °C. Band assignments of the infrared spectrum were made based upon the comparison of the infrared spectrum of FLC-3 with those of FLC-1 and FLC-2 which have very similar structures [30]. Bands at 1736 and 1715  $\text{cm}^{-1}$  are assigned to a C=O stretching mode of the core and chiral parts, respectively. Band assignments for the relevant peaks in the infrared spectrum of FLC-3 are summarized in Table I.

Figure 4 shows the infrared polarization spectra of FLC-3 in the Sm-C\* phase at the polarization angles of 15° and 105°. The direction of  $\omega = 105^\circ$  is close to the direction of the molecular long axis of FLC-3 under the external dc electric field of -40 V, and the direction of  $\omega = 15^\circ$  is close to the perpendicular direction of the molecular long axis. From these spectra the dichroic ratio  $D$ , defined as the ratio of the absorbances for the parallel and perpendicular polarizations of the radiation, was calculated for the absorption bands. The

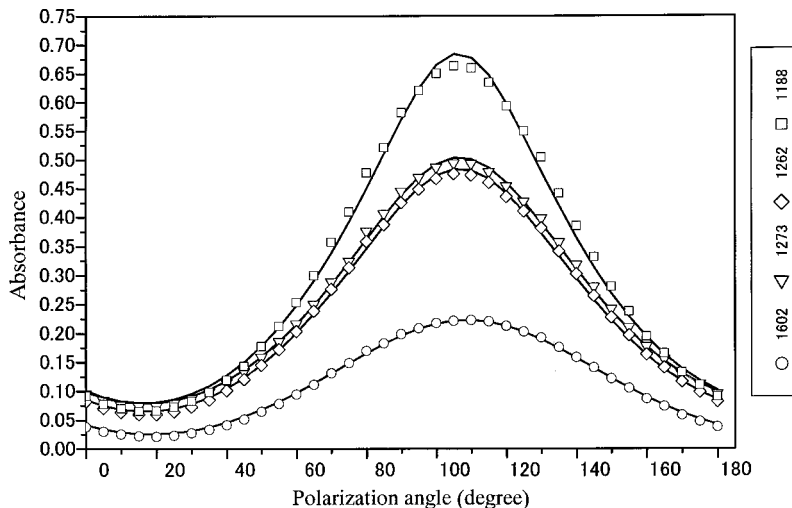


FIG. 6. The absorbance versus the polarization angle for bands at 1602, 1273, 1262, and 1188  $\text{cm}^{-1}$  in the polarized spectra of FLC-3 in the Sm-C\* phase at 137 °C under an external dc electric field of -40 V.

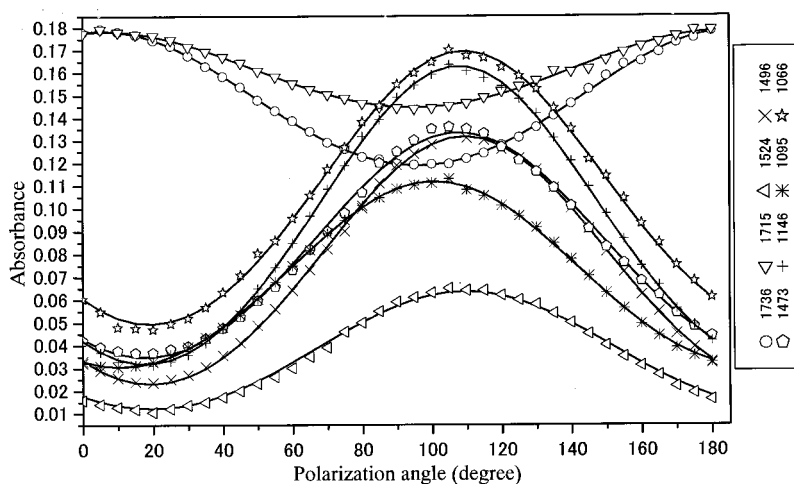


FIG. 7. The absorbance versus the polarization angle for bands at 1736, 1715, 1524, 1496, 1473, 1146, 1095, and 1066  $\text{cm}^{-1}$  in the polarized spectra of FLC-3 in the Sm-C\* phase at 137  $^{\circ}\text{C}$  under an external dc electric field of  $-40$  V.

dichroic ratios for the isolated and relevant bands are also listed in Table I. The high value of the dichroic ratio for many of the bands associated with the mesogen moiety shows that the orientational order of FLC-3 in the Sm-C\* phase is very high.

Figure 5 exhibits polarization-angle-dependent infrared spectra (from  $\omega=0^{\circ}$  to  $180^{\circ}$  at intervals of  $5^{\circ}$ ) of the sample in the Sm-C\* phase measured at 137  $^{\circ}\text{C}$  under an external dc electric field of  $-40$  V. Figure 6 shows absorbance versus polarization angle for the bands at 1602, 1273, 1262, and 1188  $\text{cm}^{-1}$ . Figure 7 shows absorbance versus polarization angle for the bands at 1736, 1715, 1524, 1496, 1473, 1146, 1095, and 1066  $\text{cm}^{-1}$ . The symbols in Figs. 6 and 7 represent measured absorbances and the curves were obtained by applying a curve fitting by a least squares method to the data.

The values of  $\alpha$  and  $\beta$  and  $S=0.748$  are obtained from the plots in Figs. 6 and 7, and  $\alpha$  and  $\beta$  are listed in Table II. From  $S=0.748$  one can conclude that the proportion of molecules in the perfectly uniaxial phase of the ferroelectric liquid crystalline system is 0.748. Simultaneously, from the dichroic ratio of the bands, we calculated the angle of orientation of the transition dipole moment with respect to the molecular long axis,  $\alpha^*$ , by the method of Ref. [28]. The

calculated values of  $\alpha^*$  are also given in Table II. The values of  $\alpha$  obtained from the curve fitting are in good agreement with the values of  $\alpha^*$ , and the maximum deviation is smaller than  $5^{\circ}$ . The standard deviation of the values of  $\beta$  is  $1.30^{\circ}$  and its average value is  $108.02^{\circ}$  for the bands with  $\alpha < 54.7^{\circ}$  except for the band at 1095  $\text{cm}^{-1}$ . A deviation of  $7.30^{\circ}$  for the band at 1095  $\text{cm}^{-1}$  is probably due to the fact that the band arises from the C-O-C group of the chiral moiety. The results in Table II suggest that the orientational direction ( $\beta$ ) of the naphthalene ring and the two benzene rings is roughly parallel to the core moiety of FLC-3. Therefore, it seems that the average orientation of the molecular long axis of FLC-3 is at an angle of  $108.02^{\circ}$  in the Sm-C\* phase at 137  $^{\circ}\text{C}$  under an external dc electric field of  $-40$  V.

Local deformations of the molecule are produced by the external dc electric field for the C=O, groups of both the core and chiral moieties in FLC-3. The deformation allows freer rotation of the molecule along its long axis. In addition, the ferroelectric liquid crystals should be able to rotate freely in the equilibrium state. The values of  $\beta$  of the bands at 1736 and 1715  $\text{cm}^{-1}$  deviate by  $12.09^{\circ}$  and  $13.13^{\circ}$ , respectively, from value for the molecular long axis. This suggests that the motion of the carbonyl groups is strongly hindered, and the distribution functions for the C=O bands are not cylindrically symmetric with respect to the molecular long axis.

Figure 8 illustrates the normalized absorbance versus the polarization angle for all bands shown in Figs. 6 and 7. The symbols in Fig. 8 represent the normalized absorbances, which were calculated according to Eq. (16). The curves were calculated according to Eqs. (17) and (18) based on the results of the curve fitting procedure. Note that some the symbols of some bands deviate from the curves. The reason is that, if the measured maximum and minimum absorbances have large deviations from the curve fitting, the normalized absorbance will be very different between the measured data and the results of the curve fitting. Therefore, when we applied the curve fitting to the data in Figs. 6 and 7, Eq. (13) but not Eqs. (17) and (18) was used to avoid a deviation from the measured data (maximum and minimum value).

In order to gain information about the angle of the molecular long axis with respect to the rubbing direction, we also measured polarization-angle-dependent infrared spectra

TABLE II.  $\alpha^*$ ,  $\alpha$ ,  $\beta$ , and  $\beta_0$ , (in deg) for infrared bands of FLO-3.

Wave number ( $\text{cm}^{-1}$ )	$\alpha^*$	$\alpha$	$\beta$	$\beta_0$
1736	62.06	61.81	95.93	4.93
1715	58.71	58.33	94.89	3.89
1602	0.00	0.46	108.80	17.80
1524	18.63	13.64	109.66	18.66
1496	19.69	14.91	109.46	18.46
1473	29.28	27.47	107.73	16.73
1273	16.48	16.49	106.72	15.72
1262	12.02	9.60	106.69	15.69
1188	5.12	6.48	106.26	15.26
1146	16.27	14.74	107.71	16.71
1095	24.11	27.07	100.72	9.72
1066	31.91	27.45	109.19	18.19

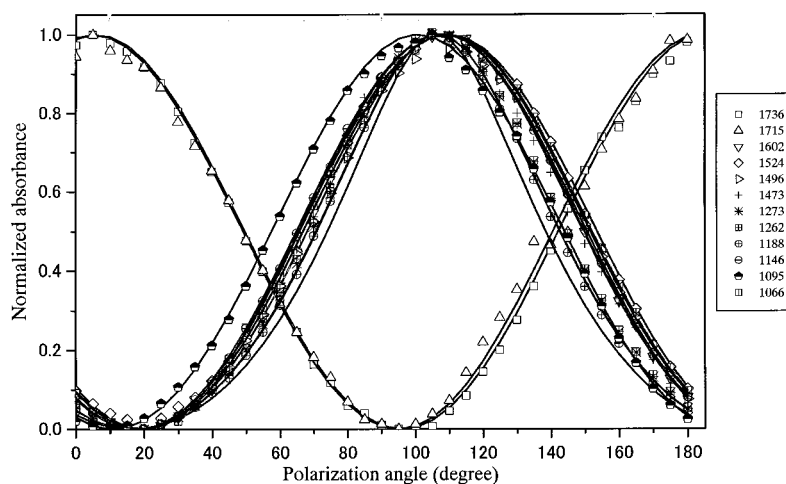


FIG. 8. Normalized absorbance versus the polarization angle for some representative bands in the polarized infrared spectra of FLC-3 in the Sm-C\* phase at 137 °C under an external dc electric field of -40 V.

of FLC-3 in the Sm-C\* phase at 137 °C under an external dc electric field of +40 V. Figure 9 depicts the normalized absorbance versus the polarization angle for the bands at 1602, 1273, and 1188  $\text{cm}^{-1}$  for both +40 and -40 V. The values of  $(\beta, \alpha)$  were calculated by the curve fitting to be  $(73.36^\circ, 0.46^\circ)$ ,  $(75.26^\circ, 16.13^\circ)$ , and  $(75.65^\circ, 5.41^\circ)$ , respectively, for the bands at 1602, 1273, and 1188  $\text{cm}^{-1}$ , and  $S=0.748$  in the Sm-C\* phase at 137 °C under an external dc electric field of +40 V. The  $\alpha$  values of these bands are nearly equal to the corresponding values in the Sm-C\* phase at 137 °C under an external dc electric field of -40 V. Ferroelectric liquid crystals perform switching between the two surface-stabilized states around the rubbing direction under an external applied electric field. Therefore, we can calculate the rubbing direction as  $91^\circ$  with respect to the polarization direction  $P_0$  (Fig. 2) from the  $\beta$  values of the bands for the electric fields with positive and negative polarity. The angle  $\beta_0$  of the molecular long axis with respect to the rubbing direction was calculated from  $\beta-91^\circ$  and is also listed in Table II. It was found that the average orientation of the molecular long axis of FLC-3 with respect to the rubbing direction is  $17.02^\circ$  for the Sm-C\* phase at 137 °C under an external dc electric field of -40 V.

The bands in the 3100–2700  $\text{cm}^{-1}$  region overlap seriously, so that the analysis of polarization-angle-dependent

spectral changes is difficult. Thus, we carried out 2D correlation analysis for the series of polarization-angle-dependent infrared spectra.

### B. Two-dimensional correlation spectroscopy

Figure 10 shows a synchronous 2D correlation spectrum in the 3020–2700  $\text{cm}^{-1}$  region, generated from the polarization-angle-dependent infrared spectra of FLC-3. Note that five autopeaks are observed at 2970, 2952, 2935, 2921, and 2854  $\text{cm}^{-1}$ . Four positive cross peaks appear at (2874 vs 2970), (2921 and 2854 vs 2952), and (2854 vs 2921)  $\text{cm}^{-1}$  and six negative cross peaks are developed at (2952, 2921, and 2854 vs 2970), (2874 vs 2952), (2874 vs 2921), and (2874 vs 2854)  $\text{cm}^{-1}$ . From the synchronous spectrum, six bands can be separated at 2970, 2952, 2935, 2921, 2874, and 2854  $\text{cm}^{-1}$ . Among these bands the two bands at 2970 and 2874  $\text{cm}^{-1}$  share the negative cross peaks with the three bands at 2952, 2921 and 2854  $\text{cm}^{-1}$ , showing that the former two bands have completely different polarization-angle dependences from the latter three bands. Therefore, the two bands at 2970 and 2874  $\text{cm}^{-1}$  may be assigned to the asymmetric and symmetric  $\text{CH}_3$  stretching modes of the chiral  $\text{CH}_3$  group. It is very likely that only this

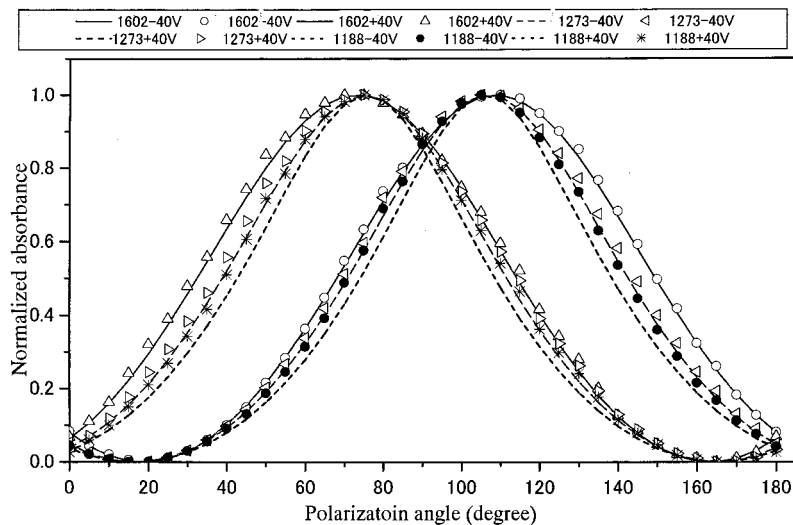


FIG. 9. Normalized absorbance versus the polarization angle for some representative bands in the polarized infrared spectra of FLC-3 in the Sm-C\* phase at 137 °C under external dc electric fields of +40 and -40 V.

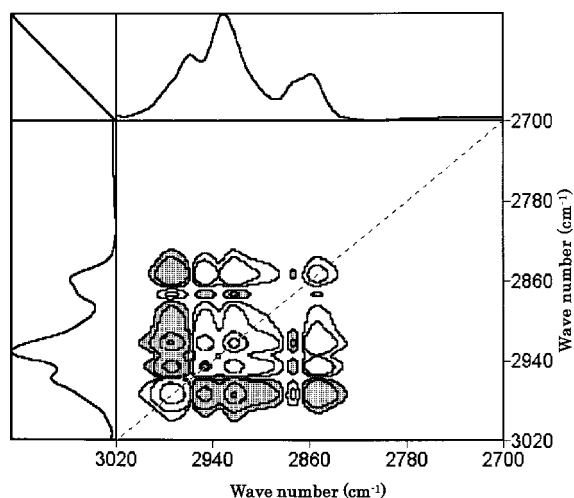


FIG. 10. Synchronous 2D infrared correlation spectrum in the 3020–2700  $\text{cm}^{-1}$  region generated from the polarization-angle-dependent (from  $0^\circ$  to  $180^\circ$  at intervals of  $5^\circ$ ) polarized spectral variations of FLC-3 in the Sm-C\* phase at  $137^\circ\text{C}$  under an external dc electric field of  $-40\text{ V}$ .

chiral  $\text{CH}_3$  group, whose transition dipole moment is in the direction of the short molecular axis, appears separately. Such information can be obtained directly via analyzing the spectra of the sample by generalized two-dimensional correlation spectroscopy. This procedure is more easily implemented in comparison with that reported previously, which requires the synthesis of two deuterated counterparts of the sample [43]. The bands at 2921 and 2854  $\text{cm}^{-1}$  are due to the antisymmetric and symmetric  $\text{CH}_2$  stretching modes of the alkyl chain, respectively. The band at 2952  $\text{cm}^{-1}$  is attributed to the asymmetric stretching mode of the  $\text{CH}_3$  groups of the alkyl chains.

Figure 11 shows the corresponding asynchronous 2D cor-

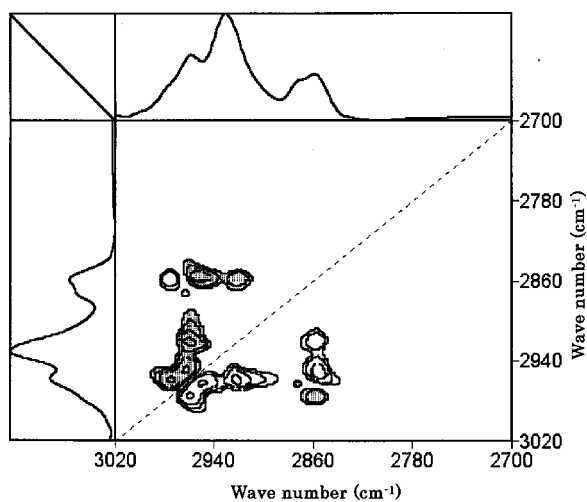


FIG. 11. Asynchronous 2D infrared correlation spectrum in the 3020–2700  $\text{cm}^{-1}$  region generated from the polarization-angle-dependent (from  $0^\circ$  to  $180^\circ$  at intervals of  $5^\circ$ ) polarized spectral variations of FLC-3 in the Sm-C\* phase at  $137^\circ\text{C}$  under an external dc electric field of  $-40\text{ V}$ .

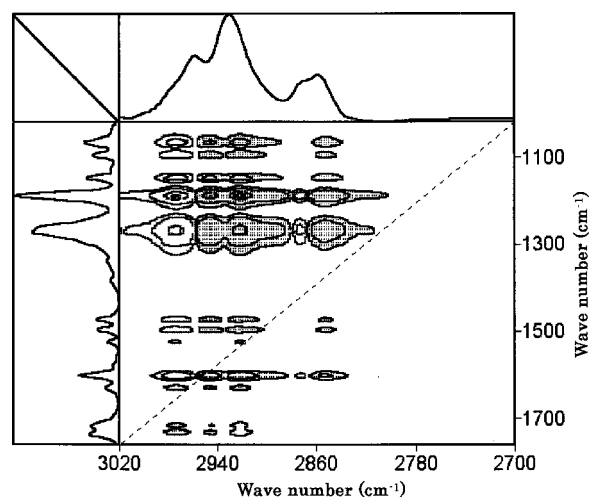


FIG. 12. Synchronous 2D infrared correlation spectrum between the 3020–2700 and 1760–1000  $\text{cm}^{-1}$  regions generated from the polarization-angle-dependent (from  $0^\circ$  to  $180^\circ$  at intervals of  $5^\circ$ ) polarized spectral variations of FLC-3 in the Sm-C\* phase at  $137^\circ\text{C}$  under an external dc electric field of  $-40\text{ V}$ .

relation spectrum in the 3020–2700  $\text{cm}^{-1}$  region. In the asynchronous spectrum are observed seven cross peaks at (2970 vs 2960 and 2854), (2960 vs 2952, 2921, and 2874), and (2854 vs 2952 and 2921)  $\text{cm}^{-1}$ . A new band can be identified at 2960  $\text{cm}^{-1}$ , and the phase of the intensity changes in the band at 2960  $\text{cm}^{-1}$  lags behind those of the bands at 2952 and 2921  $\text{cm}^{-1}$  because there are cross peaks at (2960 vs 2952 and 2921)  $\text{cm}^{-1}$ , and the sign of the cross peaks above the diagonal line is negative.

A synchronous 2D correlation spectrum between the 1760–1000 and 3020–2700  $\text{cm}^{-1}$  regions is shown in Fig. 12. It can be seen from Fig. 12 that the bands at 1627, 1602, 1524, 1496, 1473, 1262, 1188, 1146, 1095, and 1066  $\text{cm}^{-1}$  share many cross peaks with the band at 2970  $\text{cm}^{-1}$  and most of the bands in the 1630–1000  $\text{cm}^{-1}$  region. All these cross peaks between the band at 2970  $\text{cm}^{-1}$  and those in the 1630–1000  $\text{cm}^{-1}$  region always show positive sign while the cross peaks between the band at 2952 or 2921  $\text{cm}^{-1}$  and those in the 1630–1000  $\text{cm}^{-1}$  region show negative sign. However, two negative cross peaks appear between the band at 2970  $\text{cm}^{-1}$  and those at 1736 and 1715  $\text{cm}^{-1}$  and positive cross peaks are developed between the band at 2921 or 2952  $\text{cm}^{-1}$  and those at 1736 and 1715  $\text{cm}^{-1}$ . These observations suggest that the two C=O stretching bands show different polarization-angle-dependent intensity changes from the asymmetric stretching mode of the chiral  $\text{CH}_3$  group and the same polarization-angle-dependent intensity changes as the other stretching modes of the alkyl groups. Figure 13 illustrates the corresponding asynchronous spectrum where the five bands at 2970, 2960, 2952, 2921, and 2854  $\text{cm}^{-1}$  are separated. These observations are in good agreement with the results in Figs. 10 and 11.

Synchronous and asynchronous 2D correlation spectra in the 1760–1000  $\text{cm}^{-1}$  region are shown in Figs. 14 and 15, respectively. In the 1630–1450  $\text{cm}^{-1}$  region bands due to the C=C stretching modes of the three aromatic rings appear



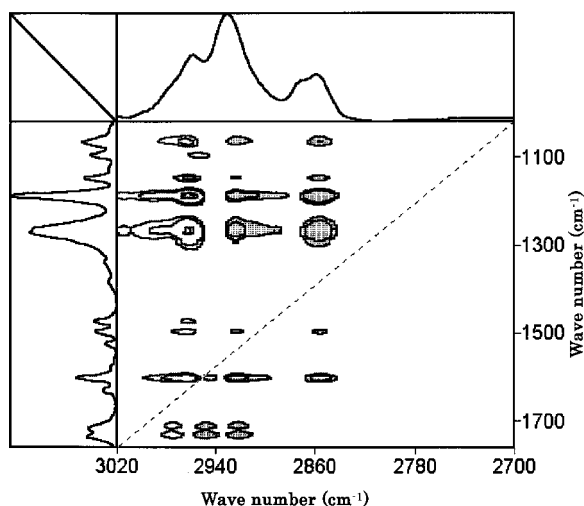


FIG. 13. Asynchronous 2D infrared correlation spectrum between the 3020–2700 and 1760–1000  $\text{cm}^{-1}$  regions generated from the polarization-angle-dependent (from  $0^\circ$  to  $180^\circ$  at intervals of  $5^\circ$ ) polarized spectral variations of FLC-3 in the Sm- $C^*$  phase at  $137^\circ\text{C}$  under an external dc electric field of  $-40$  V.

and in the 1300–1000  $\text{cm}^{-1}$  region several bands assigned to the C—O—C antisymmetric and symmetric stretching modes are observed. It seems from the synchronous spectrum that all the bands in the 1630–1000  $\text{cm}^{-1}$  region show nearly in-phase polarization-angle dependence. However, the asynchronous spectrum in Fig. 15 reveals that the phase of the intensity changes in the bands at 1602, 1524, 1496, 1473, and 1262  $\text{cm}^{-1}$  is lagging behind those in the band at 1188  $\text{cm}^{-1}$  because there are cross peaks at (1188 vs 1602, 1524, 1496, 1473, and 1262)  $\text{cm}^{-1}$ , and the sign of the cross peaks above the diagonal line is negative. From similar considerations, the following sequences of the intensity changes of bands are suggested: 1095 < 1602, 1496, 1473, 1262, 1188  $\text{cm}^{-1}$ ; 1262 < 1602, 1496  $\text{cm}^{-1}$ ; 1262, 1188 < 1066

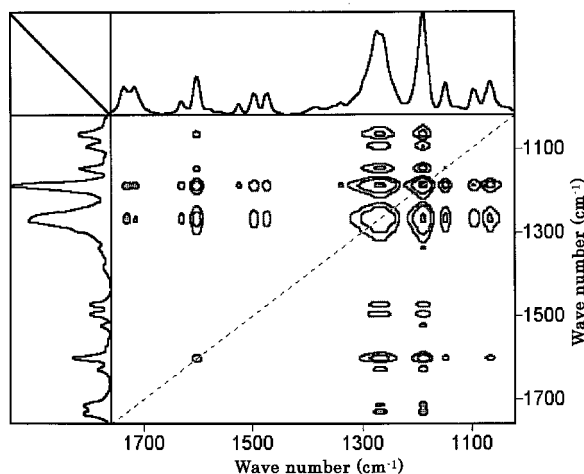


FIG. 14. Synchronous 2D infrared correlation spectrum in the 1760–1000  $\text{cm}^{-1}$  region generated from the polarization-angle-dependent (from  $0^\circ$  to  $180^\circ$  at intervals of  $5^\circ$ ) polarized spectral variations of FLC-3 in the Sm- $C^*$  phase at  $137^\circ\text{C}$  under an external dc electric field of  $-40$  V.

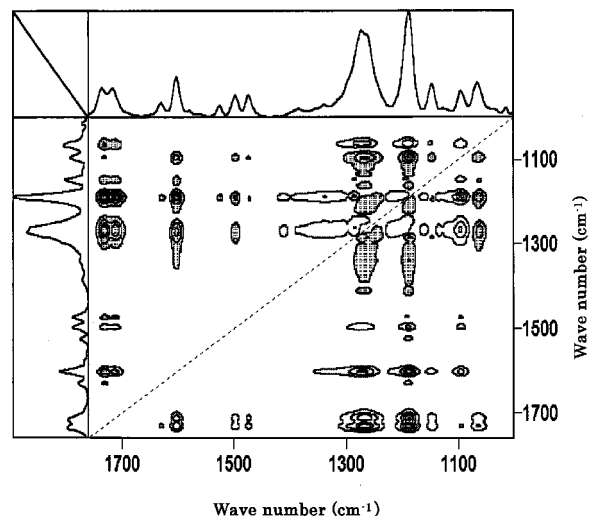


FIG. 15. Asynchronous 2D infrared correlation spectrum in the 1760–1000  $\text{cm}^{-1}$  region generated from the polarization-angle-dependent (from  $0^\circ$  to  $180^\circ$  at intervals of  $5^\circ$ ) polarized spectral variations of FLC-3 in the Sm- $C^*$  phase at  $137^\circ\text{C}$  under an external dc electric field of  $-40$  V.

$\text{cm}^{-1}$ . Thus, we may be able to conclude that the phase of the band intensity change is delayed in the order of the bands at 1095, 1188, 1262, (1496 or 1602 or 1066)  $\text{cm}^{-1}$ . This conclusion is in good agreement with the results obtained by the theoretical treatment (Table II).

## V. CONCLUSIONS

In the present paper, we proposed a theory to analyze polarization-angle-dependent infrared spectral variation of a ferroelectric liquid crystal and discussed the mutual alignment of the molecular segments of FLC-3 in the Sm- $C^*$  phase. The theory has provided the following significant information.

When  $\alpha < 54.7^\circ$ , the maximum of absorbance is in the polarization direction parallel to the direction of the molecular long axis, and we can obtain the value of the orientation angle of the molecular long axis,  $\beta$ . When  $\alpha > 54.7^\circ$ , the maximum of absorbance is in the polarization direction perpendicular to the direction of the molecular long axis, and the value of the orientation angle of the molecular long axis,  $\beta$ , can be calculated.

We have applied a curve fitting procedure to the polarization-angle-dependent changes in the band intensities. It has been found based upon the results of the curve fitting and the proposed theory that the average orientation of the molecular long axis is  $108.02^\circ$  with respect to the polarization direction  $P_0$  and  $17.02^\circ$  with respect to the rubbing direction of the cell in the Sm- $C^*$  phase at  $137^\circ\text{C}$  under an external dc electric field of  $-40$  V.

The values of  $\beta$  of the bands at 1736 and 1715  $\text{cm}^{-1}$  deviated by  $12.09^\circ$  and  $13.13^\circ$ , respectively, with respect to the average orientation of the molecular long axis. This suggests that the motion of the carbonyl groups is strongly hindered, and the distribution functions for the C=O bands are

not cylindrically symmetric with respect to the molecular long axis.

Furthermore, the present study has demonstrated the potential of 2D correlation spectroscopy in the detection of slight differences in the polarization-angle-dependent inten-

sity variations and in the band assignments for overlapping bands. The 2D correlation analysis revealed that the bands at 2970 and 2874  $\text{cm}^{-1}$  can be assigned to the asymmetric and symmetric stretching modes of the chiral  $\text{CH}_3$  group, respectively.

- 
- [1] R. B. Meyer, L. Liebert, L. Strezlecki, and P. Keller, *J. Phys. (France) Lett.* **36**, L69 (1975).
- [2] R. B. Meyer, *Mol. Cryst. Liq. Cryst.* **40**, 74 (1976).
- [3] N. A. Clark and S. T. Lagerwall, *Appl. Phys. Lett.* **36**, 899 (1980).
- [4] N. A. Clark and S. T. Lagerwall, *Ferroelectrics* **59**, 25 (1984).
- [5] S. T. Lagerwall, N. A. Clark, J. Dijon, and J. F. Clerc, *Ferroelectrics* **94**, 3 (1989).
- [6] J. S. Patel and J. W. Goodby, *Opt. Eng.* **26**, 373 (1987).
- [7] H. Toriumi, H. Sugisawa, and H. Watanabe, *Jpn. J. Appl. Phys., Part 2* **27**, L935 (1988).
- [8] V. G. Gregoriou, J. L. Chao, H. Toriumi, and R. A. Palmer, *Chem. Phys. Lett.* **179**, 491 (1991).
- [9] H. Sugisawa, H. Toriumi, and H. Watanabe, *Mol. Cryst. Liq. Cryst. Sci. Technol., Sect. A* **214**, 11 (1992).
- [10] T. Urano and H. Hamaguchi, *Chem. Phys. Lett.* **195**, 287 (1992).
- [11] T. Takano, T. Yokoyama, and H. Toriumi, *Appl. Spectrosc.* **47**, 1354 (1993).
- [12] H. Sasaki, M. Ishibashi, A. Tanaka, N. Shibuya, and R. Hasegawa, *Appl. Spectrosc.* **47**, 1390 (1993).
- [13] S. V. Shilov, S. Okretic, and H. W. Siesler, *Vib. Spectrosc.* **9**, 57 (1995).
- [14] K. Masutani, H. Sugisawa, A. Yokota, Y. Furukawa, and M. Tasumi, *Appl. Spectrosc.* **46**, 560 (1992).
- [15] K. Masutani, A. Yokota, Y. Furukawa, M. Tasumi, and A. Yoshizawa, *Appl. Spectrosc.* **47**, 1370 (1993).
- [16] M. A. Czarnecki, N. Katayama, Y. Ozaki, M. Satoh, K. Yoshio, T. Watanabe, and T. Yanagi, *Appl. Spectrosc.* **47**, 1382 (1993).
- [17] T. Urano and H. Hamaguchi, *Appl. Spectrosc.* **47**, 2108 (1993).
- [18] N. Katayama, M. A. Czarnecki, Y. Ozaki, K. Murashiro, M. Kikuchi, S. Saito, and D. Demus, *Ferroelectrics* **147**, 441 (1993).
- [19] M. A. Czarnecki, N. Katayama, M. Satoh, T. Watanabe, and Y. Ozaki, *J. Phys. Chem.* **99**, 14 101 (1995).
- [20] N. Katayama, T. Sato, Y. Ozaki, K. Murashiro, M. Kikuchi, S. Saito, D. Demus, T. Yuzawa, and H. Hamaguchi, *Appl. Spectrosc.* **49**, 977 (1995).
- [21] S. V. Shilov, S. Okretic, H. W. Siesler, R. Zentel, and T. Oge, *Macromol. Rapid Commun.* **16**, 125 (1995).
- [22] M. A. Czarnecki, S. Okretic, and H. W. Siesler, *J. Phys. Chem. B* **101**, 374 (1997).
- [23] F. Hide, N. A. Clark, K. Nito, A. Yasuda, and D. M. Walba, *Phys. Rev. Lett.* **75**, 2344 (1995).
- [24] S. V. Shilov, S. Okretic, H. W. Siesler, and M. A. Czarnecki, *Appl. Spectrosc. Rev.* **31**, 82 (1996).
- [25] K. H. Kim, K. Ishikawa, H. Takezoe, and A. Fukuda, *Phys. Rev. E* **51**, 2166 (1995).
- [26] B. Jin, Z. Ling, Y. Takanishi, K. Ishikawa, H. Takezoe, A. Fukuda, M. Kakimoto, and T. Kitazume, *Phys. Rev. E* **53**, R4295 (1996).
- [27] K. H. Kim, K. Miyachi, K. Ishikawa, H. Takezoe, and A. Fukuda, *Jpn. J. Appl. Phys., Part 1* **33**, 5850 (1994).
- [28] A. L. Verma, B. Zhao, S. M. Jiang, J. C. Shen, and Y. Ozaki, *Phys. Rev. E* **56**, 3053 (1997).
- [29] A. L. Verma, B. Zhao, H. Terauchi, and Y. Ozaki, *Phys. Rev. E* **59**, 1868 (1999).
- [30] Y. Nagasaki, T. Yoshihara, and Y. Ozaki, *J. Phys. Chem. B* **104**, 2846 (2000).
- [31] Y. Nagasaki, K. Masutani, T. Yoshihara, and Y. Ozaki, *J. Phys. Chem. B* **104**, 7881 (2000).
- [32] A. Kocot, J. K. Vij, and T. S. Perova, in *Advances in Liquid Crystals*, Vol. 113 of *Advances in Chemical Physics*, edited by J. K. Vij (Wiley, New York, 2000), pp. 213–219.
- [33] I. Noda, *Appl. Spectrosc.* **47**, 1329 (1993).
- [34] *Two-Dimensional Correlation Spectroscopy*, edited by Y. Ozaki and I. Noda, AIP Conf. Proc. No. 503 (AIP, Melville, NY, 2000).
- [35] I. Noda, in *Handbook of Vibrational Spectroscopy*, edited by C. M. Chalmers and P. R. Griffiths (Wiley, Chichester, in press).
- [36] *Appl. Spectrosc.* **54**, 236A (2000), special focus issue on two-dimensional correlation spectroscopy, edited by Y. Ozaki and I. Noda.
- [37] R. Zbinden, *Infrared Spectroscopy of High Polymers* (Academic, New York, 1964).
- [38] R. D. B. Fraser, *J. Chem. Phys.* **21**, 1511 (1953).
- [39] M. Brunet, *J. Phys. (Paris), Colloq.* **36**, C1-321 (1975).
- [40] T. Yoshihara, Y. Kiyota, H. Shiroto, T. Makino, A. Mochizuki, and H. Inoue (unpublished).
- [41] I. Noda, A. E. Dowrey, C. Marcott, Y. Ozaki, and M. G. Story, *Appl. Spectrosc.* **54**, 236 (2000).
- [42] D. Adachi, Computer program 2D POCHA, <http://science.kwansei.ac.jp/~ozaki/>.
- [43] B. Jin, S. Yoshida, Y. Takanishi, K. Ishikawa, H. Takezoe, A. Fukuda, and M. Kakimoto, *Mol. Cryst. Liq. Cryst. Sci. Technol., Sect. A* **303**, 291 (1997).